1 Production and Spectroscopy of Antihydrogen

C. Amsler, I. Johnson, N. Madsen[2], H. Pruys, C. Regenfus, and J. Rochet

in collaboration with:
CERN, University of Aarhus, Brescia, Genoa, Pavia, RIKEN, Rio de Janeiro, Swansea, Tokyo

(ATHENA Collaboration)

1.1 Introduction

Following the first observation of cold antihydrogen ($\bar{H}$) in 2002 (1), the ATHENA collaboration continued to optimize the antihydrogen formation rate and to study the $\bar{H}$ production mechanisms when low energy antiprotons are merged with dense and cold positron plasma (2)-(5). In this report we summarize the results achieved in 2004. The Zurich group has developed a new technique to measure the Lorentz deflection angle in silicon microstrip detectors (6). We have also performed a feasibility study to measure the gravitational acceleration of antimatter. Two unforeseen obstacles have been encountered by ATHENA for spectroscopy experiments with cold $\bar{H}$: first, antihydrogen appears to be formed before thermalization in the nested Penning trap that we are using. The kinetic energy is then too high to confine the $\bar{H}$ atoms in the inhomogeneous magnetic field of e.g. a quadrupole or mutipole trap. Second, the $\bar{H}$ production mechanism (radiative or three-body combination) is still ambiguous. If three-body combination dominates ($e^+e^+\bar{p} \rightarrow \bar{H}e^+$) then 1s - 2s spectroscopy is not straightforward, since this mechanism populates the high Rydberg states of the $\bar{H}$ atom. Ways are in sight to solve these issues, but this will require significant time and R & D efforts.

The ATHENA positron-antiproton mixing trap comprises a series of hollow cylinders at 15 K generating the axial (z) potential configuration of a nested Penning trap. The radial confinement is provided by a 3 T axial magnetic field. The detector for $\bar{p}$ and e^+ annihilation built by the Zurich group (7) surrounds the mixing trap. It consists of two cylindrical layers of double-sided silicon strip detectors (radii of 4 cm and 5 cm) to register the charged annihilation pions and to reconstruct the annihilation vertex. Each layer contains 16 double-sided modules with active lengths of 16 cm. Antihydrogen is detected by requiring the spatial and temporal coincidence of the vertex with two back-to-back 511 keV γ's produced by the annihilation of the positron. The γ's are detected by a high granularity electromagnetic detector comprising 192 CsI crystals with avalanche photodiode readout. A detailed description of the ATHENA apparatus can be found in ref. (8).

1.2 Measurement of the Lorentz angle

We have measured the Lorentz deflection angle in microstrip sensors operated at a temperature of 130 K in a 3 T magnetic field. This measurement was performed with cosmic ray data and the ATHENA microstrip detector. The detector axis was parallel to the homogeneous 3 T solenoidal magnetic field. Thus the charge drift is perpendicular to the magnetic field.

Due to the propagation of charge carriers along the Lorentz angle, the charge spread at the

[2]Now at the University of Aarhus, Denmark

collection surface is distorted in length and displaced. Impact positions for charged particles are reconstructed with a center of gravity algorithm of charge collected by adjacent strips. Tracks that traverse the silicon parallel to the Lorentz deflection generate the shortest charge spread and have similar charge collection properties to tracks that cross perpendicular to the sensor plane in the absence of magnetic field. A geometric model that relates the track inclination to the average cluster width has been developed to measure the Lorentz angle (6).

Cosmic rays traversing both cylinders were reconstructed from the four 3D points by requiring charged particles to fully traverse both cylinders. The four spatial measurements were fitted with a helix for data with the magnetic field on, and a straight line for data without magnetic field. The Lorentz angle was measured by fitting the model to distributions of the average cluster size as a function of track inclination. The data sample was divided into ϕ and θ intervals (polar and azimuthal angle). Three distributions are shown in Fig. 1.1. As expected, the data taken without magnetic field are symmetric around θ = 0 (perpendicular incidence), while data taken with magnetic field are shifted towards positive values. The model fits are in excellent agreement with the measuered data. These measurements correspond to holes drifting in sensors operated at 130 K in a 3 T magnetic field, and with an average internal electric field of 1.3 kV/cm. The Lorentz angle was found to be 19.6 $^{+1.0}_{-0.6}$ degrees (6).

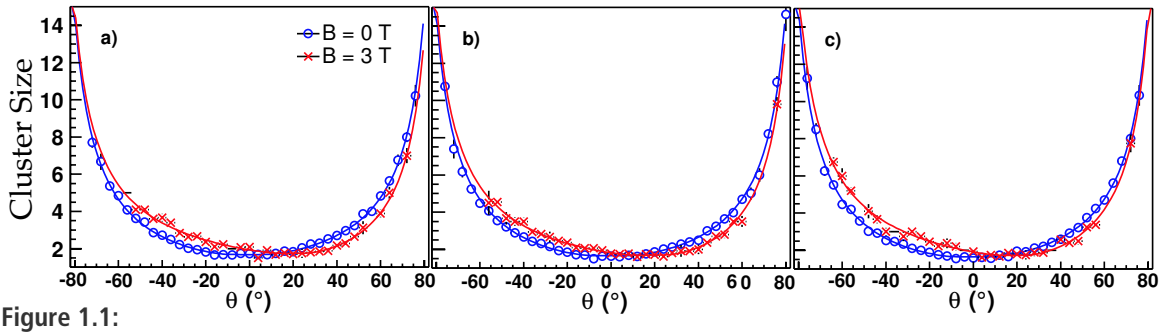

Figure 1.1:
Distribution of the average number of strips vs. inclination angle θ in three intervals of ϕ; around ϕ = -20°(a), 0° (b) and 20° (c) for field–off and field–on. The curves show the model fits.

1.3 $\bar{H}$ production mechanism

Antihydrogen production is carried out by first loading the mixing trap with 7×10^7 e^+ which cool to the ambient temperature of 15 K by the emission of synchrotron radiation, and then by injecting about 10^4 $\bar{p}$ that interact through the Coulomb interaction with the e^+ plasma. We let the antiprotons interact with the positrons for about 180 s before ejecting both species and restarting the cycle. Neutral $\bar{H}$ atoms drift towards the electrodes of the mixing trap where they annihilate.

The two relevant mechanisms for $\bar{H}$ formation are two-body radiative recombination (in which a photon removes the binding energy) and three-body combination (in which a second positron removes the excess energy). The two processes lead to different n-state populations, the former populating mainly the low n states (this is the relevant process for the 1s - 2s laser spectroscopy) and the latter mainly the high n states. The two processes have also different temperature dependences, $T^{-1/2}$ for the former and $T^{-9/2}$ for the latter. We have measured the temperature dependence of $\bar{H}$ formation (3) by changing the positron plasma temperature with a radio-frequency excitation. Neither of the two power laws gives

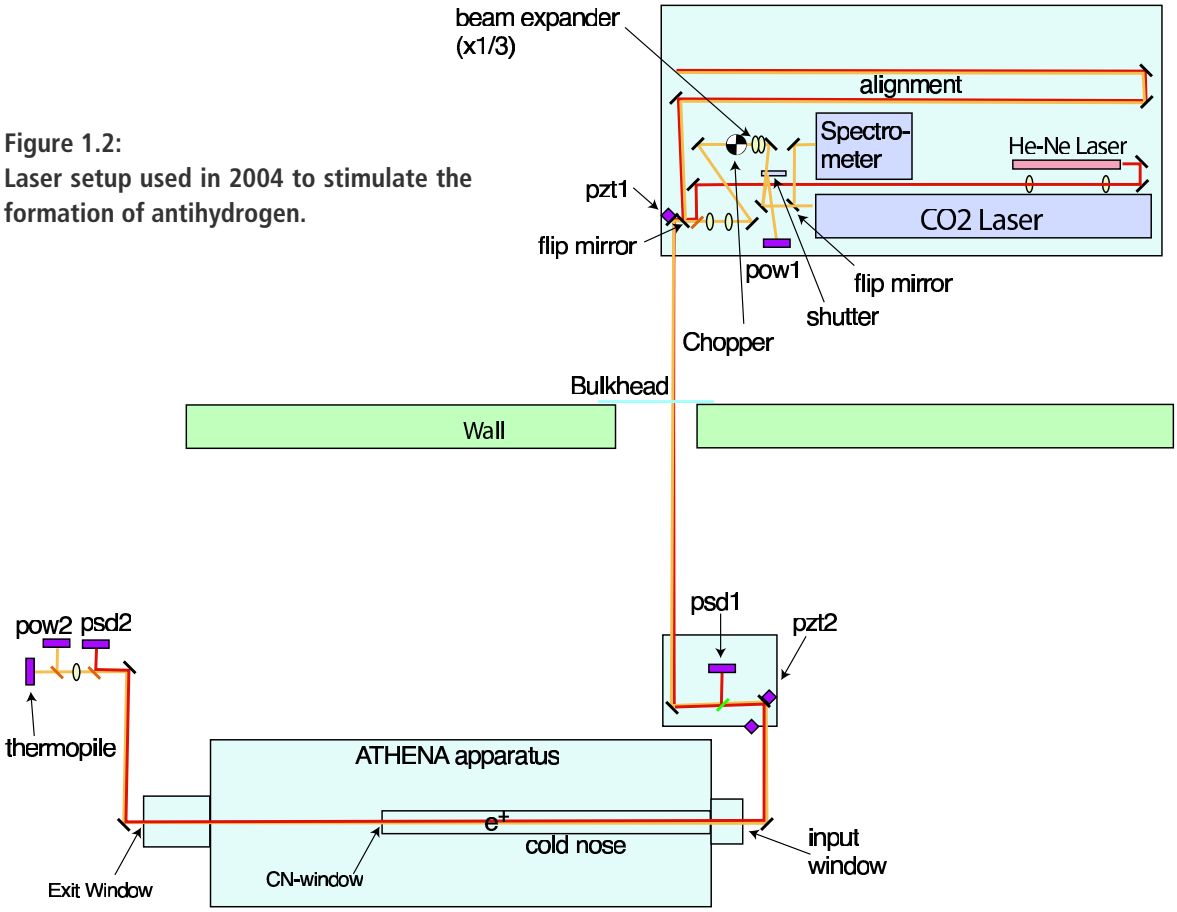

Figure 1.2:
Laser setup used in 2004 to stimulate the formation of antihydrogen.

a good fit to the data, although the $T^{-1/2}$ dependence provides a better description. Since $\bar{H}$ is still produced at room temperature, radiative combination is favored over three-body combination.

However, the observed high antihydrogen production rate (peak rate of 440 $\pm$ 40 Hz (2)) is incompatible with the much smaller rate ($<$ 40 Hz) predicted by the two-body radiative process. In fact, some recent Monte Carlo calculations based on the three-body process (9) are consistent with the observed high rate of antihydrogen production and the fraction of atoms ($\sim$ 15 %) that are sufficiently bound to escape the potential well and annihilate on the trap wall where they are detected.

Hence the cooling dynamics of the antiprotons in the mixing trap remains ambiguous and calls for more sophisticated measurements and calculations. To obtain further information on the recombination mechanism an attempt was made to stimulate radiative combination. We used a CO_2 laser to stimulate the two-body process from the continuum to the n = 11 antihydrogen bound state. The laser system in shown in Fig. 1.2. The laser beam was focused at the center of the positron cloud (beam waist 2σ = 2.0 mm). The wavelength of the laser was tuned by changing the angle of the grating which also served as the high reflecting mirror at one end of the laser cavity. The wavelength could be tuned from 9.5 μm to 11.2 μm. At the optimum wavelength of 10.96 μm the rate of stimulated two-body radiative combination was expected to be 60 Hz, a rate enhancement easily detectable by the Zurich detector. The laser power was 100 W $\cdot$ cm^{-2} and the transmission to the mixing trap 70 %, measured by a laser power meter at the end of the ATHENA main magnet, and directly at the exit of the laser.

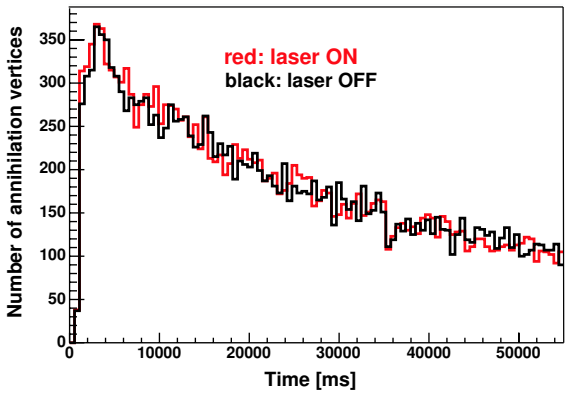

Figure 1.3:
Annihilation rate as a function of time for laser ON and laser OFF.

Figure 1.3 shows the time distribution of annihilation vertices with and without laser stimulation. There is no obvious enhancement, although the data still need to be analyzed in detail. The absence of stimulation favours the three-body recombination mechanism.

1.4 $\bar{H}$ angular distribution

We have shown that about 65 % of all observed annihilations were due to antihydrogen (2). Hence the detection of the two 511 keV γ's that led to the unambiguous observation of antihydrogen in ref. (1) (golden events) but which was inefficient ($\sim 2.5 \times 10^{-3}$) is not really required to study the production mechanism. Hence the spatial distribution of the emerging $\bar{H}$ atoms was studied without γ-coincidence to increase the size of the statistical sample (5). Figure 1.4 shows the vertex distribution along the z axis for all annihilations (a) and for $\bar{p}$ annihilations without e^+ mixing (b). Subtracting (b) from (a) (and applying a cut for the so-called hot spots in the transverse projection (10)) leads to the z distribution of annihilating $\bar{H}$ atoms (Fig. 1.4c). The distribution is in good agreement with the one obtained with the 2γ-coincidence.
Figure 1.5 shows that $\bar{H}$ atoms tend to move preferably along the z axis, although the distribution is not far from isotropy. The distribution is independent of the positron temperature (but the formation rate decreases with

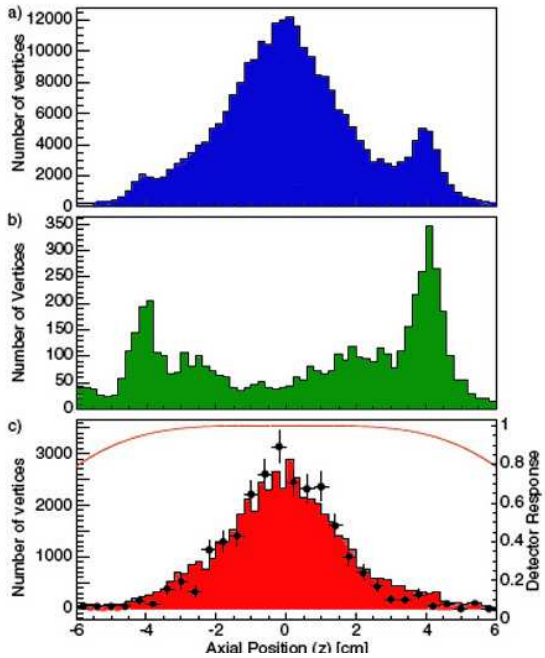

Figure 1.4:
Distribution of annihilations along the trap axis (z) (a) for all vertices during cold mixing (1.75 $\times 10^5$ events) and (b) for $\bar{p}$ annihilating in a nested trap without e^+ (5717 events). The colored area in (c) shows the difference after eliminating hot spots (4.9 $\times 10^4$ events). The full circles show $\bar{H}$ annihilations when two back-to-back 511 keV photons are required in coincidence. The solid line gives the detector acceptance.

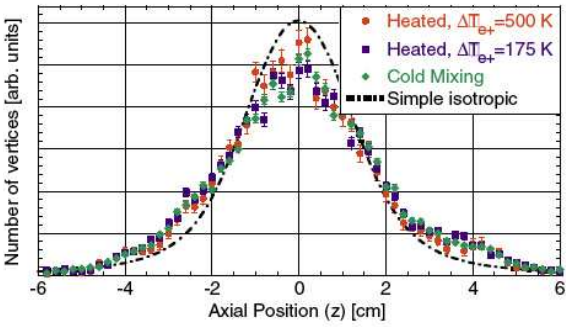

Figure 1.5:
Distribution of antihydrogen annihilation along the trap axis (z) for cold mixing and mixing with positrons heated to two different temperatures. The dot-dashed line is the prediction for isotropic emission from the positron plasma volume. The distributions have been normalized to the same area.

positron temperature). A model has been developed assuming a positron plasma rotating at a frequency of 80 kHz. The plasma was typically 2.5 mm in radius, 32 mm in length, and had a density of 1.7 $\times$ 10^8 cm^{-3}. The data in Fig. 1.5 are consistent with a two-temperature Maxwellian model for the velocities of the produced antihydrogen. In the axial direction the kinetic energy is typically an order of magnitude larger than in the transverse direction. The formation temperature is 150 K in the axial direction if the equilibrium temperature (15 K) is reached in the transverse direction. Hence antihydrogen is *not* produced at thermal equilibrium between the two plasma.

This is bad news for trapping antihydrogen and for performing $\bar{H}$ spectroscopy since typical neutral traps have depths of about 1 K. Therefore very few $\bar{H}$ will be trapped. To produce cold $\bar{H}$ it is thus necessary to have cold antiprotons before mixing with positrons.

1.5 Outlook

A possible solution to confine $\bar{H}$ could be to invert the current mechanism for formation and trap the antiprotons in the center of the nested trap, cooling them first with electrons. This means that the $e^+\bar{p} \rightarrow \bar{H}$ mechanism needs to be studied in a completely new configuration. The presence of the magnetic field gradient needed for the neutral trap also strongly influences the stability of the confinement of the charged particles. One of the major issues is the breaking of the rotational symmetry induced by the presence of the radial magnetic field having values comparable to the axial magnetic field of the charged particle trap.

The conceptual design that we are currently investigating foresees a mixing region that allows the confinement of positrons, antiprotons and the neutral antihydrogen atoms in the same volume. This is achieved by superimposing a trap for charged particle confinement with a trap for antihydrogen, made by a radial multipolar magnetic gradient together with an axial magnetic bottle. This issue is being pursued by our colleagues from Genoa with electrons and protons combining to form hydrogen. A Lyman-α laser with sufficient power for the laser cooling of antihydrogen atoms is being considered by collaborators from Florence.

1.5.1 Antimatter gravity

Assuming CPT symmetry antimatter $\bar{M}$ would fall on an anti-earth with the same acceleration g as matter M on the earth. However, CPT does not make any statement on the acceleration $\bar{g}$ of antimatter by the earth. In quantum field theories (QFT), forces mediated by the exchange of bosons with spin 1 may be repulsive or attractive (such as the γ of QED) while spin 0 and 2 exchanges are attractive. However, a QFT formulation of general relativity with a tensor T (the spin 2 graviton) is inconsistent. Extensions including supersymmetric partners of the graviton lead to vector V (spin 1) and scalar S (spin 0) exchanges. At least partial cancellation of V and S interactions is expected in MM while attractive coherence is predicted for $M\bar{M}$. Therefore antimatter will fall on earth with a larger acceleration than matter. The size of the effect depends on the relative strength between S and V exchanges. Measurements performed with Eötvös-type experiments on MM lead to predictions for the relative difference between g and $\bar{g}$ varying between 10 % and 2×10^{-6}.

We have investigated the feasibility of a pilot experiment with $\bar{H}$ atoms with energies of typically 1 K. For a 1 m flight distance the gravitational sag of a single, horizontally emitted, $\bar{H}$

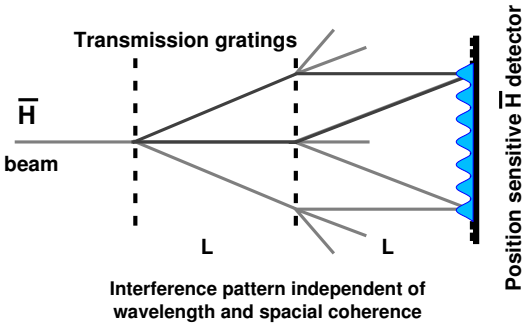

Figure 1.6:
Mach-Zehnder interferometer with two identical transmission gratings and position sensitive $\bar{H}$ detector.

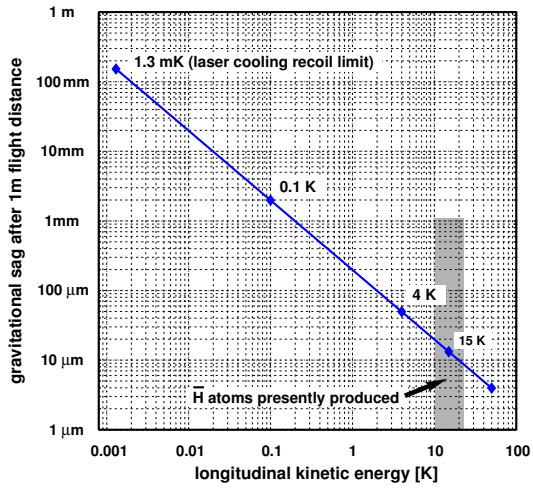

Figure 1.7:
Gravitational sag of $\bar{H}$ atoms in the gravitational field after 1 m flight distance (assuming $\bar{g}$= 9.81 m/s^2).

atom of 1 K kinetic energy could be measured to within a few percent if the emission point, initial flight direction and energy of the atom are known. Better precisions can be reached with $\bar{H}$ atoms with energies below 1 K. A possible experiment coupled to an $\bar{H}$ source would consist of horizontal slits and a position sensitive $\bar{H}$ detector to measure the sag of the interference pattern. The best solution uses a Mach-Zehnder matter wave interferometer consisting of two identical transmission gratings (Fig. 1.6). Such a device was used for measurements of g with cold atoms or neutrons (11). It does not require a monochromatic atomic source since the interference pattern is independent of wavelength. However, the divergence of the beam must be sufficiently small to avoid smearing.

The sag can be determined with high precision by rotating the setup around the beam axis by 90° (slits vertical). The gravitational sag for a distance L = 1 m is shown in Fig 1.7 as a function of temperature. A temperature of 0.5 K (typical for a multipole trap) corresponds to a sag of 400 μm.

We assume that a spatial resolution of 5 μm for the annihilation point on the detector surface can be achieved and plan to use a silicon microstrip detector detecting the $\bar{H}$ annihilations with spatial *and* time-of-flight information. The extraction of the atoms from the neutral trap could be done by either lowering one of the axial magnetic wells or kicking the $\bar{H}$ out with a magnetic pulse. Since the time of flight is in the range of 100 ms, only a moderate resolution on the kick-out time is required.

A proposal to the CERN Committees will be submitted in due time, depending on the results of the R&D efforts mentioned above. The ATHENA project itself was completed in December 2004 with the closure of the antiproton decelerator for at least 18 months.

[1] M. Amoretti *et al.* (ATHENA Collaboration), Nature **419** (2002) 456.
[2] M. Amoretti *et al.* (ATHENA Collaboration), Phys. Lett. **B 578** (2004) 23.
[3] M. Amoretti *et al.* (ATHENA Collaboration), Phys. Lett. **B 583** (2004) 59.
[4] M. Amoretti *et al.* (ATHENA Collaboration), Phys. Lett. **B 590** (2004) 133.
[5] N. Madsen *et al.* (ATHENA Collaboration), Phys. Rev. Lett. **94** (2005) 033403.
[6] I. Johnson *et al.*, Nucl. Instr. and Meth. in Phys. Res. **A 540** (2005) 113.
[7] C. Regenfus, Nucl. Instr. and Meth. in Phys. Res. **A 501** (2003) 65.
[8] M. Amoretti *et al.*, Nucl. Instr. and Meth. in Phys. Res. **A 518** (2004) 679.
[9] F. Robicheaux, Phys. Rev. **A 70** (2004) 022510.
[10] M. Fujiwara *et al.*, Phys. Rev. Lett. **92** (2004) 065005.
[11] M. Gruber *et al.*, Phys. Lett. **A 140** (1989) 363; D. W. Keith *et al.*, Phys. Rev. Lett. **66** (1991) 2693.